Possible d^0 ferromagnetism in MgO doped with nitrogen

Bo Gu,[1] Nejat Bulut,[1,2] Timothy Ziman,[3] and Sadamichi Maekawa[1,2]
[1]*Institute for Materials Research, Tohoku University, Sendai 980-8577, Japan*
[2]*JST, CREST, 3-Sanbancho, Chiyoda-ku, Tokyo 102-0075, Japan*
[3]*CNRS and Institut Laue Langevin, Boîte Postale 156, F-38042 Grenoble Cedex 9, France*
(Received 14 October 2008; published 9 January 2009)

We study the possibility of d^0 ferromagnetism in the compound MgO doped with nitrogen (N). The Haldane-Anderson impurity model is formulated within the tight-binding approximation for determining the host band structure and the impurity-host hybridization. Using the quantum Monte Carlo technique, we observe a finite local moment for an N impurity, and long-range ferromagnetic correlations between two N impurities. The ferromagnetic correlations are strongly influenced by the impurity bound state. When the ferromagnetic correlation between a pair of impurities is mapped onto the isotropic Heisenberg model for two spin-1/2 particles, the effective exchange constant J_{12} is found to increase with increasing temperature. Similar temperature dependence of J_{12} is also obtained in other diluted magnetic semiconductors, such as zincblende ZnO doped with Mn. The temperature dependence of J_{12} suggests that the mapping of the full Hamiltonian onto the spin Hamiltonian cannot fully describe the magnetic correlations for the diluted magnetic semiconductors at least in the limit of low impurity spin.

DOI: 10.1103/PhysRevB.79.024407 PACS number(s): 75.50.Pp, 75.30.Hx, 75.40.Mg

I. INTRODUCTION

There are currently a large number of observations of ferromagnetism associated with doping of *a priori* nonmagnetic species into nonmagnetic oxide semiconductors.[1–3] The subject has been given the name of d^0 magnetism to emphasize the fact that the magnetism is probably not coming from partially filled *d* orbitals, but from moments induced in the *p* orbitals of the oxygen band.[4–8] Even in cases where there are partially filled *d* orbitals, discrepancies between bulk measurements indicating ferromagnetism, and microscopic measurements by XMCD finding paramagnetic transition-metal ions, have suggested that the ferromagnetism comes from vacancies in the oxygen lattices.[9] While a fertile area of current investigation, the subject remains obscure because of problems of irreproducibility for different samples, sample inhomogeneity, stability in time, etc., and the exact origin of the magnetism is not yet established. This is unlike the case of regular diluted magnetic semiconductors such as (Ga,Mn)As,[10] where ferromagnetism is reproducible in controlled samples. The theoretical situation is also much less clear for d^0 magnetism than in the case of "classic" diluted magnetic semiconductors, where the origin of the magnetic moments, the substituted magnetic ion, is in no doubt and, in the case of Mn^{2+}, quite large ($S=5/2$). Magnetic exchange interactions leading to ferromagnetism are mediated by holes in the *p* band. For (Ga,Mn)As, Curie temperatures can be estimated with reasonable accuracy, starting from band structure to first derive the effective exchange at different distances between spins in an effective spin Hamiltonian,[11] which is then studied via classical Monte Carlo or other approximate methods.[12–14] Although this approach is adequate for bulk properties such as the ordering temperature for a variety of materials, fuller treatment of the effects of the correlation are needed for understanding more detailed properties such as the local densities of states and impurity band structure.[15] Even for thermodynamic properties such as the Curie temperature, there is good reason to doubt straightforward application of methods apparently working for "classic" diluted magnetic semiconductors to the materials that may show d^0 magnetism. In this case, the induced moments postulated in the oxygen bands are not fully localized, but are formed by the same holes that generate effective exchange. It was recently argued, for example, that[16] because of this, exchanges estimated from local approximations, such as the local spin-density approximation (LSDA) may consistently overestimate the tendency for ferromagnetism and even formation of local moments, compared to extensions, such as self-interaction correction (SIC). Thus much of the theoretical literature may be overoptimistic in predictions of ferromagnetism, even at zero temperature. One can even question whether the approach is valid to first project the full Hamiltonian onto the zero-temperature spin Hamiltonian, to which the effects of thermal fluctuations are added.

It is important, therefore, to develop methods which treat correlations correctly and that do not rely on arbitrary approximations or on the separation between spin and charge fluctuations. Such a method has been introduced and applied to models of the "classic" diluted magnetic semiconductors,[17–19] namely Quantum Monte Carlo (QMC) methods based on the Hirsch-Fye algorithm. These can directly give spin correlations at finite temperatures without making any assumption of projection onto an effective Hamiltonian. In this paper we apply the method to an interesting case of possible d^0 magnetism, namely, MgO diluted with nitrogen. Our aim is then to answer, by means of Quantum Monte Carlo methods, the following questions. First, does such an unbiased calculation predict ferromagnetic (FM) correlations in such a material? Second, of more general interest, do the standard approaches, as described above, still apply? In fact ferromagnetism has previously been predicted at low concentrations[20] in the doped alkaline-earth metal oxides (MgO, CaO, BaO, and SrO) doped with N and C. Our results are not completely comparable to those results, in that we shall consider a simpler model Hamiltonian

for the host and two impurities only, rather than a finite concentration. We should be able to draw useful general conclusions both for the particular material and the methods.

II. FERROMAGNETIC CORRELATIONS BETWEEN TWO N IMPURITIES

A. Impurity model

In order to describe N impurities in MgO host, we take the two-step calculations. First, the Haldane-Anderson impurity model[21] is formulated within the tight-binding approximation for determining the host band structure and the impurity-host hybridization. Second, the magnetic correlations of the Haldane-Anderson impurity model at finite temperatures are calculated by the Hirsch-Fye quantum Monte Carlo technique.[22]

The Haldane-Anderson impurity model is defined as

$$H = \sum_{\mathbf{k},\alpha,\sigma} [\epsilon_\alpha(\mathbf{k}) - \mu] c^\dagger_{\mathbf{k}\alpha\sigma} c_{\mathbf{k}\alpha\sigma} + \sum_{\mathbf{k},\alpha,\mathbf{i},\xi,\sigma} (V_{\mathbf{i}\xi\mathbf{k}\alpha} p^\dagger_{\mathbf{i}\xi\sigma} c_{\mathbf{k}\alpha\sigma} + \text{H.c.}) + (\epsilon_p - \mu) \sum_{\mathbf{i},\xi,\sigma} p^\dagger_{\mathbf{i}\xi\sigma} p_{\mathbf{i}\xi\sigma} + U \sum_{\mathbf{i},\xi} n_{\mathbf{i}\xi\uparrow} n_{\mathbf{i}\xi\downarrow}, \quad (1)$$

where $c^\dagger_{\mathbf{k}\alpha\sigma}$ ($c_{\mathbf{k}\alpha\sigma}$) is the creation (annihilation) operator for a host electron with wavevector $\mathbf{k}$ and spin σ in the valence ($\alpha=v$) or conduction ($\alpha=c$) band, and $p^\dagger_{\mathbf{i}\xi\sigma}$ ($p_{\mathbf{i}\xi\sigma}$) is the creation (annihilation) operator for a localized electron at impurity site $\mathbf{i}$ in orbital ξ ($\xi=x,y,z$) and spin σ with $n_{\mathbf{i}\xi\sigma} = p^\dagger_{\mathbf{i}\xi\sigma} p_{\mathbf{i}\xi\sigma}$. Here, $\epsilon_\alpha(\mathbf{k})$ is the host band dispersion, μ is the chemical potential, $V_{\mathbf{i}\xi\mathbf{k}\alpha}$ is the mixing between the impurity and host, ϵ_p is the impurity $2p$ orbital energy, and U is the on-site Coulomb repulsion for the impurity.

The energy bands $\epsilon_\alpha(\mathbf{k})$ for MgO host and the impurity-host hybridization $V_{\mathbf{i}\xi\mathbf{k}\alpha}$ will be calculated within the tight-binding approximation. For a large number of simple oxides, the on-site Coulomb repulsion energy of holes in an oxygen p orbital is 5–7 eV.[5] For the on-site Coulomb repulsion of $2p$ orbitals at an N impurity site in the compound MgO, the experimental value is unknown so here we take it as $U=6$ eV. In addition, the experimental value of impurity $2p$ energy ϵ_p(N) in Mg(O,N) is also unknown. In the following, we use ϵ_p(N) as the parameter satisfying $\epsilon_p(\mathrm{N}) > \epsilon_p(\mathrm{O}) = -2.03$ eV, where the value of ϵ_p(O) is taken from the tight-binding parameters for the compound MgO (see below).

For the compound Mg(O,N), there is one $2p$ hole at an N^{2-} site so it is reasonable to neglect the Hund couplings among different $2p$ orbitals at an N^{2-} site.

B. Tight-binding approach for the MgO band structure and the N-MgO hybridization

In this section, we discuss the tight-binding calculation for the MgO band structure and the hybridization between an N impurity and MgO host. For MgO with rocksalt structure, the band structure $\epsilon_\alpha(\mathbf{k})$ had already been calculated with a set of tight-binding parameters.[23] In this approach, the basis consists of a $3s$ orbital for the cation Mg^{2+} and three degenerate $2p$ orbitals for the anion O^{2-}. The orbital energies are ϵ_s(Mg)=9.88 eV and ϵ_p(O)=−2.03 eV. In addition, the

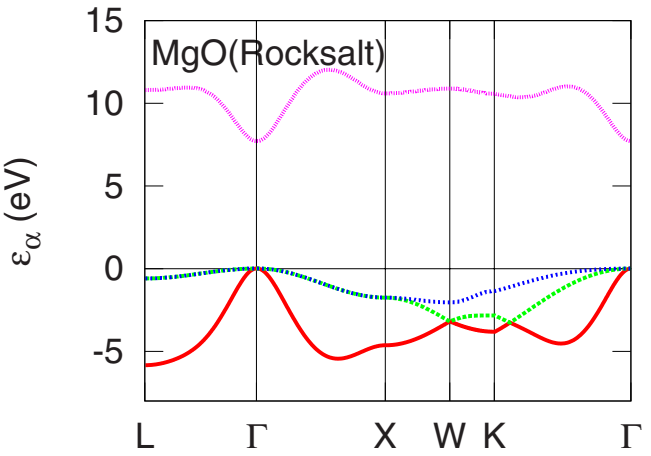

FIG. 1. (Color online) Energy bands of MgO with rocksalt crystal structure. These results were reproduced using the tight-binding parameters in Ref. 23, where one $3s$ orbital of Mg and three $2p$ orbitals of O are included.

mixing values between the s orbital of Mg^{2+} and the p orbitals of O^{2-} up to the third-nearest neighbors are taken to be $(sp\sigma)_1=1.10$ eV, $(ss\sigma)_2=-0.18$ eV, $(pp\sigma)_2=0.65$ eV, $(pp\pi)_2=-0.07$ eV, and $(sp\sigma)_3=0.89$ eV, where $(\,)_n$ means the mixing of the nth nearest neighbors. Using these tight-binding parameters, we have reproduced the band structure of rocksalt MgO as shown in Fig. 1, where band structure consists of one conduction band and three valence bands. The conduction band mainly comes from $3s$ orbital of Mg, and valence bands mainly come from $2p$ orbitals of O. The top of valence bands and the bottom of conduction band are located at the Γ point with a direct gap of 7.72 eV.

Next, we discuss the calculation of the hybridization between N impurity and MgO host within the tight-binding approximation. The hybridization matrix element $V_{\mathbf{i}\xi\mathbf{k}\alpha} \equiv \langle \varphi_\xi(\mathbf{i}) | H | \Psi_\alpha(\mathbf{k}) \rangle$ has the form of

$$V_{\mathbf{i}\xi\mathbf{k}\alpha} = \frac{1}{\sqrt{N}} e^{i\mathbf{k}\cdot\mathbf{i}} \sum_{o,\mathbf{n}} e^{i\mathbf{k}\cdot(\mathbf{n}-\mathbf{i})} a_{\alpha o}(\mathbf{k}) \langle \varphi_\xi(\mathbf{i}) | H | \varphi_o(\mathbf{n}) \rangle \equiv \frac{1}{\sqrt{N}} e^{i\mathbf{k}\cdot\mathbf{i}} V_{\xi\alpha}(\mathbf{k}), \quad (2)$$

where $\varphi_\xi(\mathbf{i})$ is the impurity $2p$ state ($\xi=x,y,z$) at site $\mathbf{i}$, and $\Psi_\alpha(\mathbf{k})$ is the host state with wavevector $\mathbf{k}$ and band index α, which is expanded by atomic orbitals $\varphi_o(\mathbf{n})$ with orbital index o and site index $\mathbf{n}$. Here, N is the total number of host-lattice sites, and $a_{\alpha o}(\mathbf{k})$ is an expansion coefficient. For the mixing integrals of $\langle \varphi_\xi(\mathbf{i}) | H | \varphi_o(\mathbf{n}) \rangle$, ξ denotes the three $2p$ orbitals of N^{2-}, and o represents the $3s$ orbital of Mg^{2+} and $2p$ orbitals of O^{2-}. As shown by Slater and Koster,[24] these mixing integrals up to the third-nearest neighbors can be expressed by four integrals $(sp\sigma)_1$ $(pp\sigma)_2$, $(pp\pi)_2$, and $(sp\sigma)_3$, and direction cosines l, m, and n in the two-center approximation, where $(\,)_n$ means the mixing of the nth nearest neighbors. As the experimental values of the above four integrals are unknown, here we take these mixing integrals between N and MgO as the same mixing values between O and MgO in Ref. 23. Thus, we have $(sp\sigma)_1=1.10$ eV,

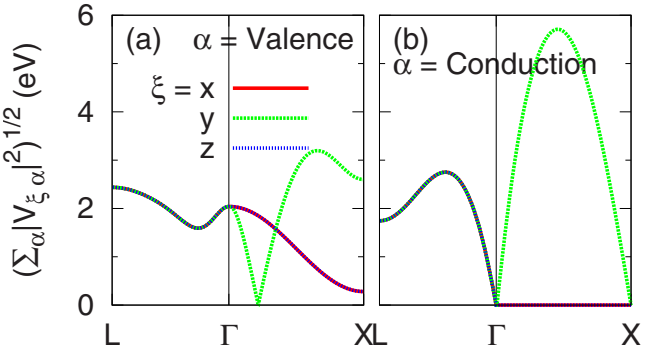

FIG. 2. (Color online) Hybridization function $\bar{V}_\xi(\mathbf{k})$ between ξ orbital of an N impurity and MgO host (a) valence bands or (b) conduction band. Here, the mixing parameters between N and MgO are taken as the same mixing values between O and MgO in Ref. 23.

$(pp\sigma)_2$=0.65 eV, $(pp\pi)_2$=−0.07 eV, and $(sp\sigma)_3$=0.89 eV for the impurity-host hybridization.

Figure 2 displays results on the impurity-host mixing function $\bar{V}_\xi(\mathbf{k})$ defined by

$$\bar{V}_\xi(\mathbf{k}) \equiv \left(\sum_\alpha |V_{\xi\alpha}(\mathbf{k})|^2 \right)^{1/2} \tag{3}$$

where ξ is a $2p(x,y,z)$ orbital of an N impurity. In Eq. (3), the summation over α is performed only over the valence bands [Fig. 2(a)] or the conduction band [Fig. 2(b)]. Here, $\bar{V}_\xi(\mathbf{k})$ is plotted along various directions in the Brillouin zone for rocksalt crystal structure. It is observed that, at the Γ point, the total hybridization between the ξ orbital of an N impurity and the MgO valence bands is finite, while that with the MgO conduction band is zero. For the host MgO, the gap edge is located at the Γ point, hence the value of $\bar{V}$ near Γ will be particularly important in determining the energy of the impurity bound state, which may appear in the gap due to the mixing between impurity and host.

C. Quantum Monte Carlo results

In this section, we present results on the magnetic correlations of the Haldane-Anderson impurity model obtained by the Hirsch-Fye QMC technique.[22] The parameters related to the MgO host and N impurity have been calculated within the tight-binding approach described above. The following results were obtained with more than 10^5 Monte Carlo sweeps and Matsubara time step $\Delta\tau$=0.225.

We first discuss the local-moment formation for an N impurity in the MgO host. For this purpose, we have performed QMC simulations to calculate $\langle (M^z)^2 \rangle$, where

$$M^z = n_{\mathbf{i}\xi\uparrow} - n_{\mathbf{i}\xi\downarrow} \tag{4}$$

is the magnetization operator for a ξ orbital of an N impurity at site $\mathbf{i}$. Figure 3 shows $\langle (M^z)^2 \rangle$ versus the chemical potential μ at temperature T=200 K, where $0<\mu<0.5$ eV. As mentioned before, the experimental value of impurity $2p$ energy $\epsilon_p(N)$ in Mg(O,N) is not known so it is taken as a parameter satisfying the relation $\epsilon_p(N)>\epsilon_p(O)$=−2.03 eV.

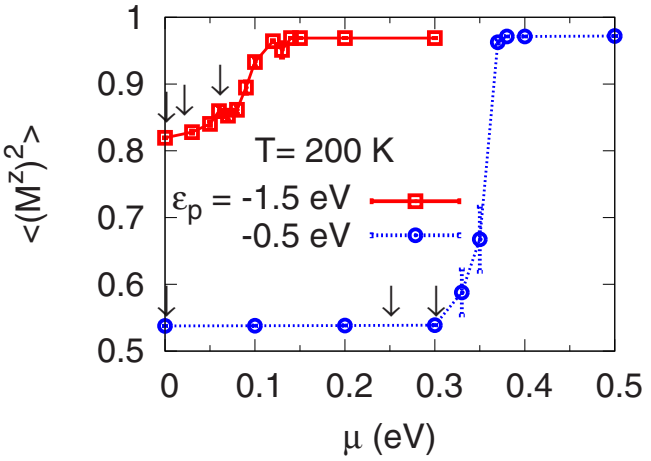

FIG. 3. (Color online) Square of magnetic moment $\langle (M^z)^2 \rangle$ of an N impurity versus chemical potential μ at T=200 K. The experimental value of impurity $2p$ energy $\epsilon_p(N)$ in Mg(O,N) is unknown, but it should satisfy the relation $\epsilon_p(N)>\epsilon_p(O)$=−2.03 eV. Here, the arrows indicate the different position of μ investigated by Fig. 4.

As shown in Fig. 3, the sharp increases in the magnitude of the magnetic moment are observed around 0.08 and 0.35 eV for the impurity $2p$ energy ϵ_p=−1.5 eV and ϵ_p=−0.5 eV, respectively. In our model $2p$ orbitals are degenerate, and thus the calculated curves in Fig. 3 do not change with ξ =x, y, or z. In addition, no such sharp increases (or sharp decreases) are observed near the bottom of the conduction band. As shown in Fig. 2, the values of the hybridization with bottom of conduction band are around zero and thus much weaker than those with top of valence bands.

According to the Hartee-Fock[25] and QMC calculations,[17–19] the presence of a sharp increase (or a sharp decrease) in $\langle (M^z)^2 \rangle$ versus μ implies the existence of an impurity bound state (IBS) at this energy, and the IBS plays an important role in determining the strength of the FM correlations. When the IBS is unoccupied, FM correlations can develop between the impurities. When the IBS is occupied, the FM correlations become weaker.

When two N impurities are introduced in the MgO host, they can replace any two O positions in the rocksalt lattice MgO. Let us then briefly explain how our QMC calculations of the magnetic correlations function $\langle M_1^z M_2^z \rangle$ actually proceed with the different spatial positions of the two impurities. When the position of the two impurities changes, the corresponding hybridization $V_{\mathbf{i}\xi\mathbf{k}\alpha}$, including the impurity spatial position $\mathbf{i}$ as defined in Eq. (2), will change; the Green's function between impurity 1 and impurity 2, including the factor $V^*_{1\xi\mathbf{k}\alpha} V_{2\xi\mathbf{k}\alpha}$, will change; and thus the magnetic correlations function $\langle M_1^z M_2^z \rangle$ changes. See Ref. 26 for more details of the QMC calculations.

The magnetic correlation function $\langle M_1^z M_2^z \rangle$ between ξ=x orbitals of the impurities versus the impurity separation R/a at temperature T=200 K is shown in Fig. 4. The direction $R \| (0.5,0,0.5)$ is chosen to be along one of the 12 nearest N-N neighbors in rocksalt structure, and a is the lattice constant. Results in Fig. 4(a) are obtained with fixed impurity energy ϵ_p=−1.5 eV for various chemical potential μ. The

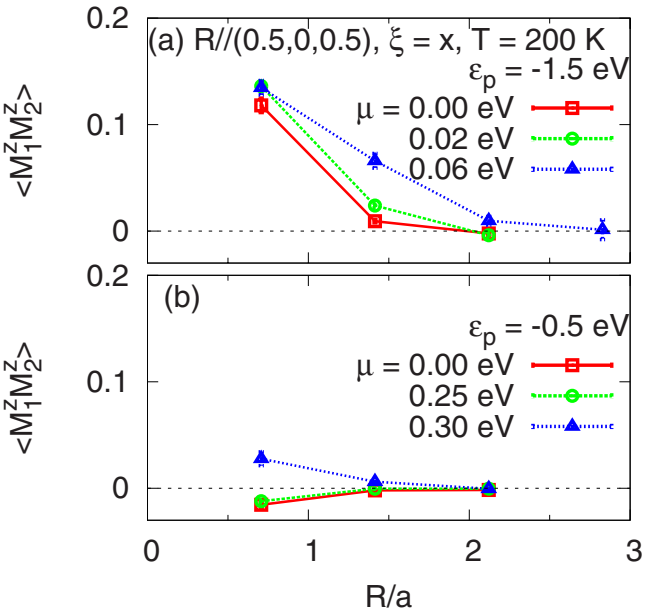

FIG. 4. (Color online) Magnetic correlation function $\langle M_1^z M_2^z \rangle$ between $\xi=x$ orbitals of the N impurities versus distance R/a for (a) the impurity $2p$ energy $\epsilon_p=-1.5$ eV and (b) $\epsilon_p=-0.5$ eV at $T=200$ K. Direction $R\|(0.5,0,0.5)$ is along one of the 12 nearest N-N neighbors in rocksalt structure.

impurity spins exhibit FM correlations at chemical potential $\mu=0.0$ eV. It is noted that the IBS of Mg(O,N) lies near 0.08 eV in the gap, close to the top of the valence band as displayed in Fig. 3. By increasing μ to 0.06 eV, the FM correlations become larger, and the range of the FM correlations becomes longer. Further increasing μ, the FM correlations become weaker. This is because the IBS of Mg(O,N) becomes occupied when μ is increased to above 0.06 eV, as seen in Fig. 3. Results in Fig. 4(b) are obtained with fixed impurity energy $\epsilon_p=-0.5$ eV for various values of the chemical potential μ. The impurity spins exhibit quite weak antiferromagnetic (AFM) correlations due to the superexchange interaction at $\mu=0.0$ eV. It is worth pointing out that the IBS of Mg(O,N) lies around 0.35 eV, deep in the band gap as shown in Fig. 3. Increasing μ to 0.3 eV, the FM correlations appear with stronger magnitude and longer range. Further increasing μ to above 0.3 eV, the FM correlations become weaker. This is because the IBS of Mg(O,N) is occupied when $\mu>0.3$ eV, as displayed in Fig. 3.

In the direction $R\|(0.5,0,0.5)$, let us discuss the correlation function $\langle M_1^z M_2^z \rangle$ between other orbitals of two N impurities in the MgO host. Considering the symmetry in the direction $R\|(0.5,0,0.5)$, $\langle M_1^z M_2^z \rangle$ between $\xi=z$ orbitals of two N impurities have the same value between $\xi=x$ orbitals of two N impurities. For the $\langle M_1^z M_2^z \rangle$ between $\xi=y$ orbitals of two N impurities in the direction $R\|(0.5,0,0.5)$, our QMC calculations (not present here) show that it is short-range FM correlation. For the nearest N-N neighbors distance $R=(0.5,0,0.5)a$ in the case that $\epsilon_p=-1.5$ eV, $\mu=0.06$ eV, and $T=200$ K, the magnetic correlation function $\langle M_1^z M_2^z \rangle$ between different ξ orbitals is shown in Fig. 5. It is found that the magnetic correlations between different orbitals of two N impurities are much smaller than the values between the same orbitals.

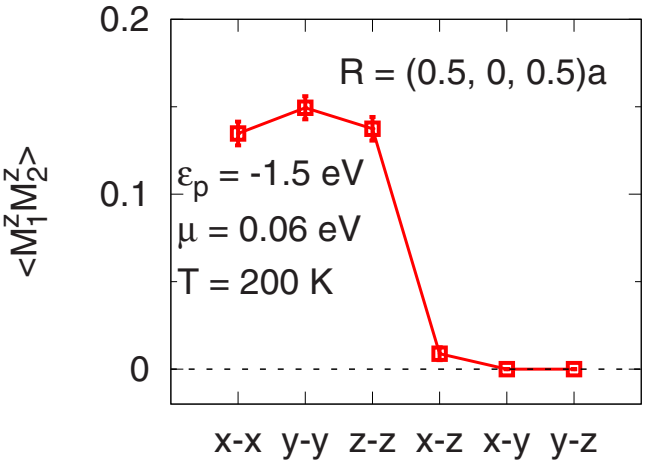

FIG. 5. (Color online) Magnetic correlation function $\langle M_1^z M_2^z \rangle$ between $2p$ orbitals of two N impurities. Distance $R=(0.5,0,0.5)a$ is one of the 12 nearest N-N neighbors in rocksalt structure. Here, $\epsilon_p=-1.5$ eV, $\mu=0.06$ eV, and $T=200$ K.

For the two N impurities in the MgO host, there are 12 nearest N-N neighbors in rocksalt structure: $(0,\pm0.5,\pm0.5)a$, $(\pm0.5,0,\pm0.5)a$, and $(\pm0.5,\pm0.5,0)a$. For the direction R along other 11 nearest N-N neighbors, $\langle M_1^z M_2^z \rangle$ of two N impurities could be got by symmetry without calculation. For example, $\langle M_1^z M_2^z \rangle$ between $\xi=x$ orbital of two N impurities in direction $R\|(0,0.5,0.5)$ is the same value as that between $\xi=y$ orbitals of two N impurities in direction $R\|(0.5,0,0.5)$. Thus, for $\epsilon_p=-1.5$ eV and $\mu=0.06$ eV, the long-range FM correlation between two N impurities could be observed at $T=200$ K along all of the 12 nearest N-N neighbors in rocksalt Mg(O,N).

The calculations presented above do not include the Jahn-Teller (JT) distortion, which might occur in the compound Mg(O,N). As the JT distortion is included, the energy level of x, y, and z orbitals of the impurity N will differ, being higher for some orbitals and being lower for the others, but the values changed are often quite small. As a result, the IBS shown in Fig. 3 will differ for different p orbitals, being shallower in the gap for those having lower energy level and being deeper in the gap for those having higher energy level, and again the shift values of the IBS will be quite small. More importantly, the long-range FM correlations, as shown in Fig. 4, will become stronger for those having the shallower IBS and become weaker for those having the deeper IBS, and of course the change will be quite small. So, here we argue that the JT distortion will play a quite small role in our calculations.

III. MAPPING OF FERROMAGNETISM ONTO A HEISENBERG MODEL

The ferromagnetic correlation between two N impurities is mapped onto the isotropic Heisenberg model for two spin-1/2 particles

$$H=-J_{12}\mathbf{M}_1\cdot\mathbf{M}_2. \tag{5}$$

At finite temperature, defining $\beta=1/k_BT$ with k_B the Boltzmann constant, the impurity-impurity correlation is defined as

$$\langle M_1^z M_2^z \rangle = \mathrm{Tr}(M_1^z M_2^z e^{-\beta H})/\mathrm{Tr}(e^{-\beta H}).$$

Considering

$$\mathbf{M}_1 \cdot \mathbf{M}_2 = \frac{1}{2}[(\mathbf{M}_1 + \mathbf{M}_2)^2 - \mathbf{M}_1^2 - \mathbf{M}_2^2]$$

$$= \frac{1}{2}[S(S+1) - 2s(s+1)],$$

where $s=1/2$, $S=0,1$, and the trace here could be taken as

$$\mathrm{Tr}(\cdots) = \sum_{S^z=-S}^{S} \sum_{S=0}^{1} (\cdots) = \sum_{s_2^z=-1/2}^{1/2} \sum_{s_1^z=-1/2}^{1/2} (\cdots),$$

we have

$$\langle M_1^z M_2^z \rangle = \frac{1}{4} \cdot \frac{1 - e^{-\beta J_{12}}}{3 + e^{-\beta J_{12}}},$$

where the unit of $\langle M_1^z M_2^z \rangle$ is $1^2=(2s)^2=(2\mu_B)^2$ and μ_B is Bohr magneton. To be consistent with our QMC calculation results, whose unit of $\langle M_1^z M_2^z \rangle$ is μ_B^2, the above equation is modified as

$$\langle M_1^z M_2^z \rangle = \frac{1 - e^{-\beta J_{12}}}{3 + e^{-\beta J_{12}}}. \tag{6}$$

Thus, inverting this relation, we can deduce an effective exchange coupling J_{12} between two N impurities from

$$J_{12} = k_B T \ln \frac{1 + \langle M_1^z M_2^z \rangle}{1 - 3\langle M_1^z M_2^z \rangle}. \tag{7}$$

Figure 6 shows the temperature dependence of the magnetic correlation function $\langle M_1^z M_2^z \rangle$ and the corresponding exchange coupling J_{12} between $\xi=x$ orbitals of two N impurities. Here, the following parameters are taken as $\epsilon_p=-1.5$ eV, $\mu=0.06$ eV, $R=(0.5,0,0.5)a$, or $R=(1,0,1)a$. For the two N impurities with distance $R=(0.5,0,0.5)a$, it is found that with increasing temperature from 200 to 400 K, magnetic correlation function $\langle M_1^z M_2^z \rangle$ decreases, but the exchange coupling J_{12} increases. For the two N impurities with distance $R=(1,0,1)a$, the temperature dependence of exchange coupling J_{12} becomes weaker.

For $\langle M_1^z M_2^z \rangle$ and J_{12} between $\xi=y$ or z orbitals of two N impurities in the direction $R \| (0.5,0,0.5)$, the similar behaviors are observed. For the direction R along other 11 nearest N-N neighbors, the behaviors of temperature dependence could be found by symmetry without calculation as discussed in the last section. Thus, with $\epsilon_p=-1.5$ eV and $\mu=0.06$ eV, the temperature dependence of $\langle M_1^z M_2^z \rangle$ and J_{12} between two N impurities, as shown in Fig. 6, could be observed along all of the 12 nearest N-N neighbors in rocksalt Mg(O,N).

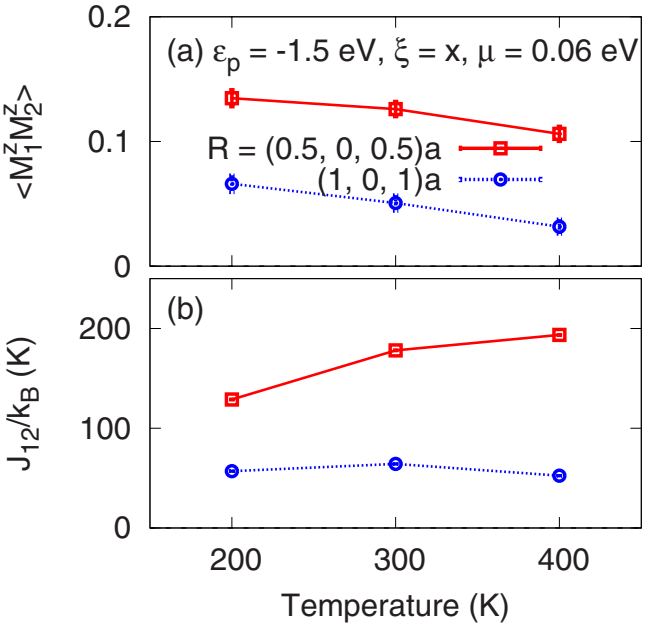

FIG. 6. (Color online) Temperature dependence of (a) the magnetic correlation function $\langle M_1^z M_2^z \rangle$ between x orbitals of two N impurities and (b) corresponding exchange coupling J_{12} calculated by Eq. (7). Here, $\epsilon_p=-1.5$ eV, $\mu=0.06$ eV, $R=(0.5,0,0.5)a$, or $R=(1,0,1)a$.

IV. DISCUSSION

To understand the long-range FM correlation function $\langle M_1^z M_2^z \rangle$ between two N impurities in MgO host, as shown in Fig. 4, which is mediated by the impurity-induced polarization of the host electron spins, it is more convenient to study the local density of states in real space around the impurity. Here we have considered the impurity-host correlation function $\langle M^z m^z(\mathbf{r}) \rangle$ and the number of polarized host electrons $\langle n(\mathbf{r}) - n(\infty) \rangle$ for the case of one-impurity N in the MgO host. Here, $\mathbf{r}$ is the site of host electron and the impurity N is located at site $\mathbf{r}=0$. In addition, $n(\infty)$ means the number of host electrons at infinity distance, thus $\langle n(\mathbf{r}) - n(\infty) \rangle$ is negative and represents the number of holes. The magnetization $m^z(\mathbf{r})$ and number $n(\mathbf{r})$ operators are defined as

$$m^z(\mathbf{r}) = \sum_{\alpha} (n_{\alpha \mathbf{r}\uparrow} - n_{\alpha \mathbf{r}\downarrow}), \tag{8}$$

$$n(\mathbf{r}) = \sum_{\alpha} (n_{\alpha \mathbf{r}\uparrow} + n_{\alpha \mathbf{r}\downarrow}), \tag{9}$$

where $n_{\alpha \mathbf{r}\sigma}=c_{\alpha \mathbf{r}\sigma}^{\dagger} c_{\alpha \mathbf{r}\sigma}$ is the number operator for host electrons with band index α and site $\mathbf{r}$ and spin σ. With impurity $2p$ energy $\epsilon_p=-1.5$ eV and chemical potential $\mu=0.06$ eV and direction $\mathbf{r} \| (0.5,0,0.5)$, the long-range AFM correlation between x orbital of N impurity and MgO host is observed in Fig. 7(a), and the polarized host electrons with long-range distribution are also observed in Fig. 7(b). As the holes in the valence band around the impurity N are spin-polarized, the valence band is spin polarized. Comparing Fig. 4(a) with Fig. 7(a), it is confirmed that the long-range AFM impurity-host correlations contribute to the long-range FM impurity-impurity correlations. With increasing temperature, as shown in Fig. 7(a), the magnitude of AFM impurity-host correlation function $\langle M^z m^z(\mathbf{r}) \rangle$ decreases, which induces the decreasing FM impurity-impurity correlation function $\langle M_1^z M_2^z \rangle$ with increasing temperature as shown in Fig. 6(a).

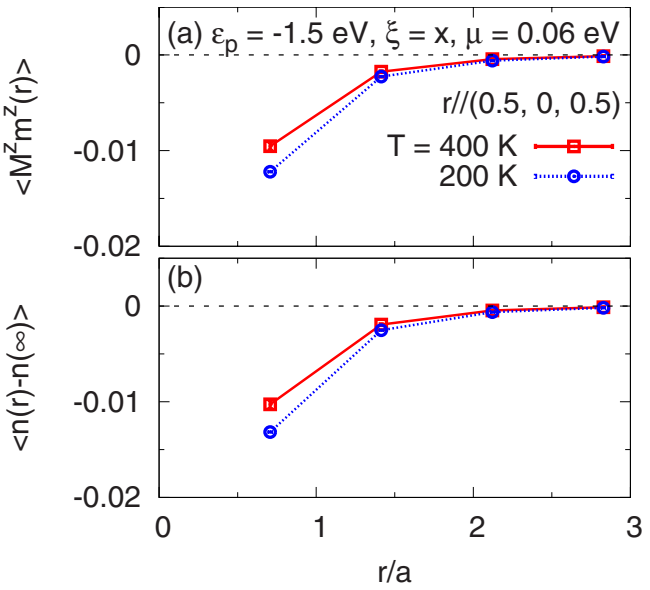

FIG. 7. (Color online) Spatial variation in (a) the magnetic correlation function $\langle M^z m^z(r)\rangle$ between x orbital of an N impurity and MgO host, and (b) the number of polarized host electrons $\langle n(r)-n(\infty)\rangle$. Here, $\epsilon_p=-1.5$ eV, $\mu=0.06$ eV, and $r\|(0.5,0,0.5)$.

To understand the temperature-dependent exchange coupling J_{12} shown in Fig. 6(b), we have studied a "classic" diluted magnetic semiconductor, zincblende ZnO doped with Mn. As shown in Fig. 8, a similar temperature-dependent exchange coupling J_{12} is obtained. Here, magnetic correlation function $\langle M_1^z M_2^z\rangle$ between xy orbitals of two Mn impurities is calculated, and the corresponding exchange coupling J_{12} is given by Eq. (7). Because the experimental value of ϵ_d for Mn in ZnO host is unknown, here we use the symmetric case of $\epsilon_d=-U/2+\mu$ so that the impurity sites develop large magnetic moments. For the compound (Zn,Mn)O, the value of the on-site Coulomb repulsion for Mn^{2+} is taken as $U=5.2$ eV by comparing with the photoemission spectroscopy measurements.[27] The chemical-potential value $\mu=0.1$ eV is set close to the impurity bound state. The direction $R\|(0.5,0,0.5)$ is chosen to be along one of the 12 nearest Mn-Mn neighbors in zincblende structure. We find that the exchange constant J_{12} increases with increasing temperature as was the case in Mg(O,N).

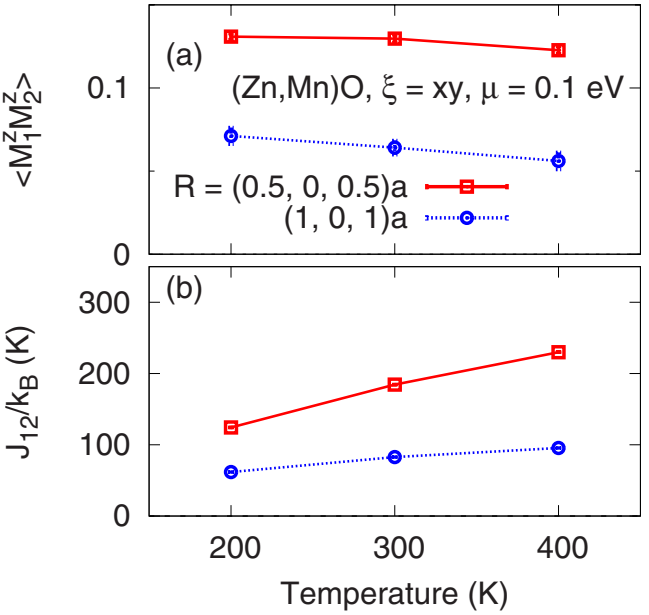

FIG. 8. (Color online) For zincblende ZnO doped with Mn, temperature dependence of (a) the magnetic correlation function $\langle M_1^z M_2^z\rangle$ between xy orbitals of two Mn impurities and (b) the corresponding effective exchange coupling J_{12} calculated by Eq. (7). Here $\epsilon_d=-U/2+\mu$, $\mu=0.1$ eV, and $R\|(0.5,0,0.5)$

We have to note that our result of J_{12} does indeed contradict the common assumption that people make when using the Lichtenstein formula, but here we are dealing with a low-spin situation, in contrast to what is usually (but not always) done in the literature. Thus our results are most pertinent for d^0 situations, and the results for zincblende ZnO doped with Mn are in fact based on an effective spin-1/2 model.

V. SUMMARY AND CONCLUSIONS

In summary, we have studied possible d^0 ferromagnetism for the compound Mg(O,N) in the dilute impurity limit based on the Haldane-Anderson impurity model. The band structures of the MgO host were calculated using the tight-binding approach. The mixing parameters between N and MgO are approximated as being the same as between O and MgO. The QMC results show the development of a large magnetic moment at an N impurity site, and long-range ferromagnetic correlations between two N impurities. The ferromagnetic correlation between impurity pairs is mapped onto the isotropic Heisenberg model for two spin-1/2 particles, and the effective exchange coupling J_{12} for given separation of impurities is found to increase with increasing temperature. Similar temperature dependence of J_{12} is also obtained in "classic" diluted magnetic semiconductors, such as zincblende ZnO doped with Mn, suggesting that the mapping is not fully valid even there at least in the limit of low impurity spin. For the particular case of MgO doped with N the results presented in this paper, in which no such approximation is made and in which interactions are treated exactly, suggest that there should be stable moments associated with each impurity and that they should have ferromagnetic correlations. While the results are for two impurities only, the long range of the correlations suggests long-range ferromagnetic order for low concentrations.

Note added in proof. We wish to point out recent publications for MgO:N (Ref. [7]) and the closely related SrO:N (Ref. [8]) suggesting formation of moments, within the framework of LDA-U, and consistent with the experimental spectra of SrO:N.

ACKNOWLEDGMENTS

This work was supported by the NAREGI Nanoscience Project, a Grant-in-Aid for Scientific Research from the Ministry of Education, Culture, Sports, Science and Technology

of Japan, and NEDO. The authors thank the Supercomputer Center at the Institute for Solid State Physics, University of Tokyo, for the use of the facilities. T.Z. thanks the International Frontier Center for Advanced Materials of Tohoku University and the members of the IMR for their support of his stay in Sendai, which enabled this collaboration. The authors acknowledge S. Parkin for valuable discussions about the experiment of Mg(O,N).

[1] M. Venkatesan, C. B. Fitzgerald, and J. M. D. Coey, Nature (London) **430**, 630 (2004).
[2] M. Venkatesan, C. B. Fitzgerald, J. G. Lunney, and J. M. D. Coey, Phys. Rev. Lett. **93**, 177206 (2004).
[3] J. M. D. Coey, M. Venkatesan, P. Stamenov, C. B. Fitzgerald, and L. S. Dorneles, Phys. Rev. B **72**, 024450 (2005).
[4] A. M. Stoneham, A. P. Pathak, and R. H. Bartram, J. Phys. C **9**, 73 (1976).
[5] I. S. Elfimov, S. Yunoki, and G. A. Sawatzky, Phys. Rev. Lett. **89**, 216403 (2002).
[6] C. Das Pemmaraju and S. Sanvito, Phys. Rev. Lett. **94**, 217205 (2005).
[7] I. S. Elfimov, A. Rusydi, S. I. Csiszar, Z. Hu, H. H. Hsieh, H.-J. Lin, C. T. Chen, R. Liang, and G. A. Sawatzky, Phys. Rev. Lett. **98**, 137202 (2007).
[8] V. Pardo and W. E. Pickett, Phys. Rev. B **78**, 134427 (2008).
[9] T. Tietze, M. Gacic, G. Schtz, G. Jakob, S. Brck, and E. Goering, N. J. Phys. **10**, 055009 (2008).
[10] H. Ohno, Science **281**, 951 (1998).
[11] A. I. Liechtenstein, M. I. Katsnelson, V. P. Antropov, and V. A. Gubanov, J. Magn. Magn. Mater. **67**, 65 (1987).
[12] L. Bergqvist, O. Eriksson, J. Kudrnovsky, V. Drchal, P. Korzhavyi, and I. Turek, Phys. Rev. Lett. **93**, 137202 (2004).
[13] K. Sato, W. Schweika, P. H. Dederichs, and H. Katayama-Yoshida, Phys. Rev. B **70**, 201202(R) (2004).
[14] G. Bouzerar, T. Ziman, and J. Kudrnovsky, Europhys. Lett. **69**, 812 (2005).
[15] J. Ohe, Y. Tomoda, N. Bulut, R. Arita, K. Nakamura, and S. Maekawa, arXiv:0812.0430 (unpublished).
[16] A. Droghetti, C. D. Pemmaraju and S. Sanvito, Phys. Rev. B **78**, 140404(R) (2008).
[17] N. Bulut, K. Tanikawa, S. Takahashi, and S. Maekawa, Phys. Rev. B **76**, 045220 (2007).
[18] Y. Tomoda, N. Bulut, and S. Maekawa, arXiv:0806.0095 (unpublished).
[19] B. Gu, N. Bulut, and S. Maekawa, J. Appl. Phys. **104**, 103906 (2008).
[20] K. Kenmochi, V. A. Dinh, K. Sato, A. Yanase, and H. Katayama-Yoshida, J. Phys. Soc. Jpn. **73**, 2952 (2004); V. A. Dinh, M. Toyoda, K. Sato, and H. Katayama-Yoshida, *ibid.* **75**, 093705 (2006).
[21] F. D. M. Haldane and P. W. Anderson, Phys. Rev. B **13**, 2553 (1976).
[22] J. E. Hirsch and R. M. Fye, Phys. Rev. Lett. **56**, 2521 (1986).
[23] V. C. Lee and H. S. Wong, J. Phys. Soc. Jpn. **45**, 895 (1978).
[24] J. C. Slater and G. F. Koster, Phys. Rev. **94**, 1498 (1954).
[25] M. Ichimura, K. Tanikawa, S. Takahashi, G. Baskaran, and S. Maekawa, in *Foundations of Quantum Mechanics in the Light of New Technology*, edited by S. Ishioka and K. Fujikawa (World Scientific, Singapore, 2006), pp. 183–186; arXiv:cond-mat/0701736 (unpublished).
[26] R. M. Fye, J. E. Hirsch, and D. J. Scalapino, Phys. Rev. B **35**, 4901 (1987).
[27] T. Mizokawa, T. Nambu, A. Fujimori, T. Fukumura, and M. Kawasaki, Phys. Rev. B **65**, 085209 (2002).